

Supporting Information

Structure optimization of prussian blue analogue cathode materials for advanced sodium ion batteries

Dezhi Yang,^a Jing Xu,^a Xiao-Zhen Liao,^{*a} Yu-Shi He,^a Haimei Liu^b and Zi-Feng Ma^{*a}

^a Institute of Electrochemical and Energy Technology, Department of Chemical Engineering, Shanghai Jiao Tong University, Shanghai 200240, China. Fax: +86 21 5474 1297; Tel: +86 21 5474 2894; E-mail: zfma@sjtu.edu.cn; liaoxz@sjtu.edu.cn

^b College of Environmental and Chemical Engineering, Shanghai University of Electric Power, Shanghai 200090, China

S1. Experimental

PBMN was synthesized by mixing 200mL of 0.08M Na₄Fe(CN)₆ solution and 200mL mixed solution containing 0.01 M NiCl₂ and 0.05 M MnCl₂ drop by drop to 1000mL H₂O under continuous stirring. PBN was prepared by mixing 200mL of 0.05M Na₄Fe(CN)₆ solution and 200mL of 0.04 M NiCl₂ solution drop by drop under continuous stirring. PBM was prepared as the same with PBN that mixing Na₄Fe(CN)₆ and MnCl₂ solution. The synthesized precipitates (PBMN, PBN, PBM) were filtered, washed with water and then dried in vacuum at 100 °C. The synthetic process should run at dark environment to avoid lighting induced redox action of Fe(CN)₆⁴⁻/Fe(CN)₆³⁻ and lighting induced decomposition of Fe(CN)₆ group. The hard carbon was acquired from Sumitomo Bakelite Co., Ltd.

For a typical coin cell fabrication, the cathodes were prepared by slurring 70wt.% active material (PBMN, PBN or PBM), 20wt.% super P, and 10wt.% polyvinylidene fluoride (PVDF) in N-methyl-2-pyrrolidone (NMP), and then casting the mixture onto an aluminum foil. After vacuum drying at 80°C for about 4h, the electrode disks (14 mm) were punched and weighed. The cathode active material loading was 3-4 mg cm⁻². After further drying under vacuum at 120 °C for 12 h, the cathodes were incorporated into coin cells (R2016) with sodium metal foil and 1.0M NaClO₄/EC+DMC (1:1, v/v)

electrolyte in an argon filled glove box. The advanced sodium ion batteries were assembled of PBMN cathode, hard carbon anode and 1.0M NaClO₄/EC+DMC (1:1, v/v) electrolyte, and then packaged with aluminum plastic film in an argon-filled glove box. The PBMN cathode consisted of 70wt.% PBMN, 20wt.% super P, and 10wt.% PVDF. The hard carbon anode consisted of 80wt.% hard carbon, 10wt.% super P, and 10wt.% PVDF. The loadings of cathode active material and anode active material were 3-4 mg cm⁻² and 5-6 mg cm⁻², respectively.

The structural characteristic of the as-prepared materials were determined by X-ray diffraction (XRD, D/max-2200/PC, Rigaku Co., Ltd.) with filtered Cu K α radiation. X-ray photoelectron spectroscopy (XPS, Kratos Axis Ultra-DLD, Kratos Analytical) was obtained with a monochromatic Al K α radiation source. The binding energies of all elements were calibrated to that of carbon (284.6 eV). The morphologies of the samples were analyzed by scanning electron microscopy (SEM, Sirion 200, FEI Company). The chemical composition was examined by the elemental analysis (EA, Vario-EL Cube, Elementar Analysensysteme) for C and N elements, and by inductively coupled plasma analysis (ICP, iCAP 6000 Radial, Thermo Fisher Scientific Inc.) for Fe, Ni, Mn and Na elements. The thermo gravimetric (TG) analysis was conducted on a DSC/DTA-TG instrument (TG, STA 449 F3 Jupiter, NETZSCH-Gerätebau GmbH) at 2 °C min⁻¹ heating rate of under N₂ environment.

The galvanostatic charge-discharge test was conducted using a battery test system (Land CT2001A model, Wuhan Jinnuo Electronics Co., Ltd.). All cyclic voltammetric experiments were performed on CHI electrochemical workstation (CHI 670D, CHI Instrument Co.). All electrochemical experiments were carried out at 25 °C.

S2. The thermo gravimetric (TG) analysis of PBM, PBN and PBMN

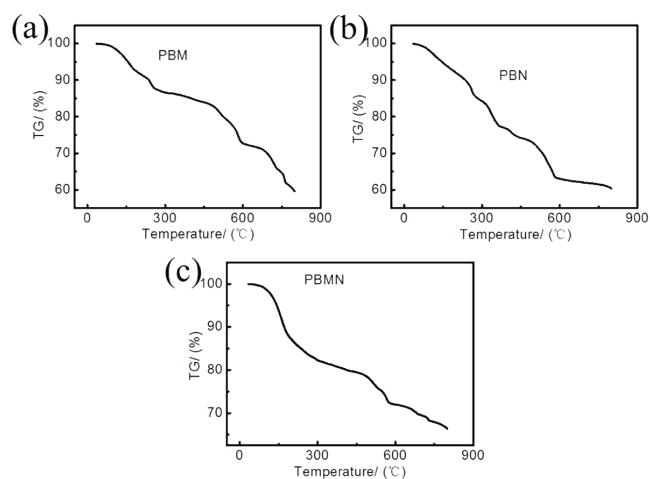


Figure S1. The thermo gravimetric (TG) curves of PBM (a), PBN (b) and PBMN (c) under N₂ environment.

S3. The structure schematic of PBMN

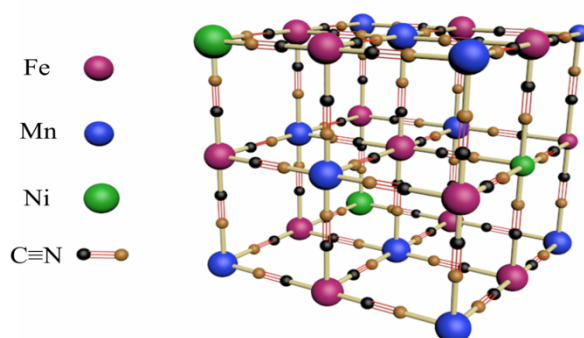


Figure S2. The structure schematic of PBMN.

S4. The XPS survey spectrums of PBMN

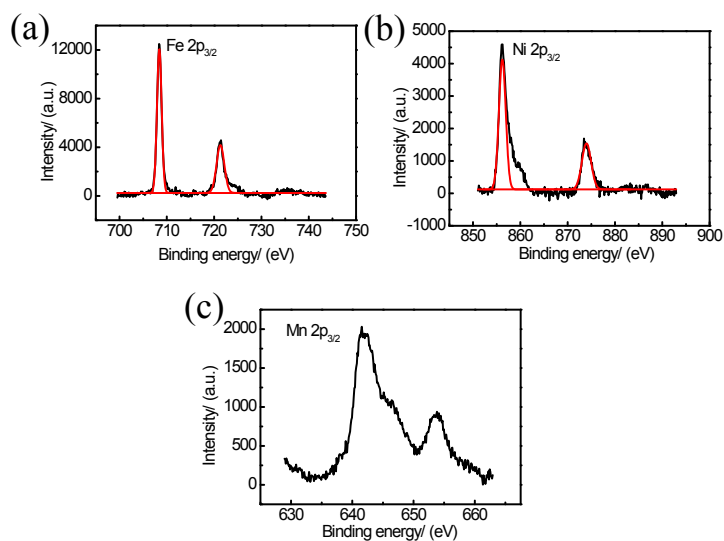


Figure S3. XPS spectra of PBMN for the (a) Fe 2p_{3/2}, (b) Ni 2p_{2/3} and (c) Mn 2p_{2/3} spectral region. The red line is fitting results of the peaks.

S5. The SEM images of PBMN electrode after 800 charge/discharge cycles

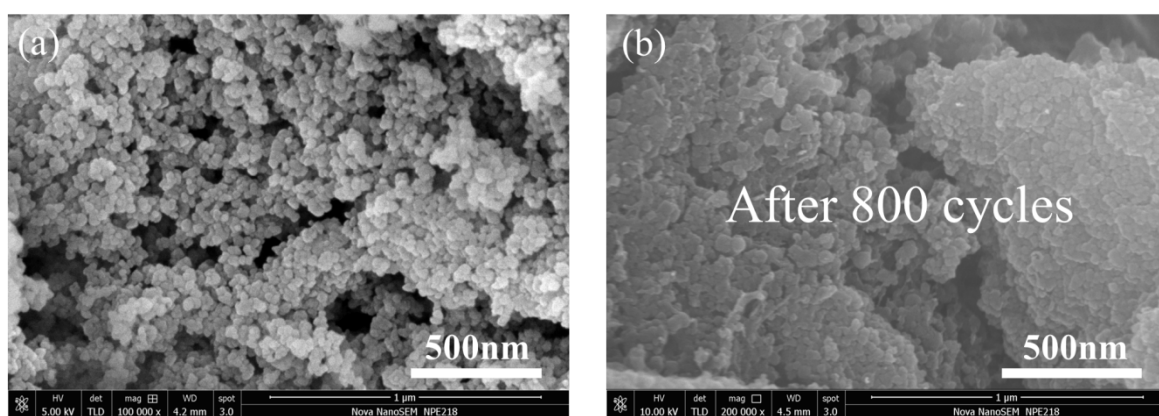


Figure S4. SEM images of PBMN (a) and PBMN electrode (b) after 800 charge/discharge cycles.

S6. The X-ray diffraction patterns of PBMN electrode after 800 charge/discharge cycles

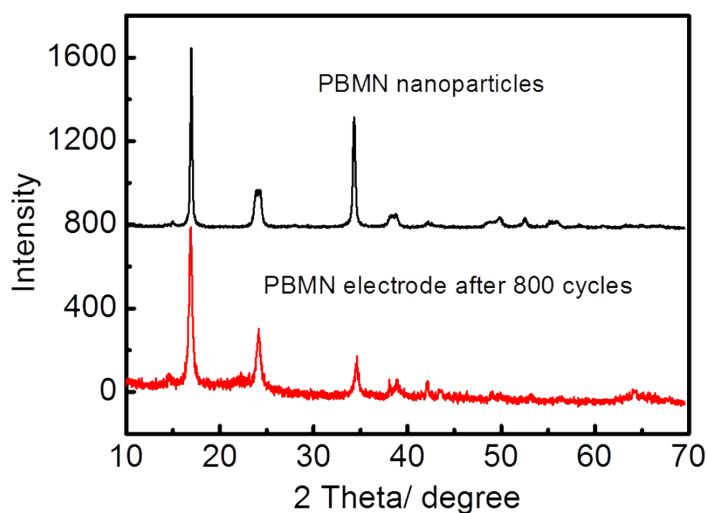


Figure S5. X-ray diffraction patterns of PBMN and PBMN electrode after 800 charge/discharge cycles (Background peaks have been excluded).

S7. The cycle performances of PBMNs with different Ni content

As shown in Fig. S6, after 800 cycles, the capacity retentions of $\text{Na}_{1.76}\text{Ni}_{0.12}\text{Mn}_{0.88}\text{Fe}(\text{CN})_6$, $\text{Na}_{1.81}\text{Ni}_{0.48}\text{Mn}_{0.52}\text{Fe}(\text{CN})_6$ and $\text{Na}_{1.84}\text{Ni}_{0.76}\text{Mn}_{0.24}\text{Fe}(\text{CN})_6$ were 83.78%, 84.93% and 87.31%, with first discharge capacities of 96.97 mAh/g, 80.57 mAh/g and 61.6 mAh/g, respectively. With increased Ni content in the PBMN, the discharge capacity was significantly decreased but the cycle stability was increased in small ranges. Taking both the specific capacity and cycle stability into consideration, we chose the $\text{Na}_{1.76}\text{Ni}_{0.12}\text{Mn}_{0.88}\text{Fe}(\text{CN})_6$ sample to prepare the soft packed sodium ion battery in this paper.

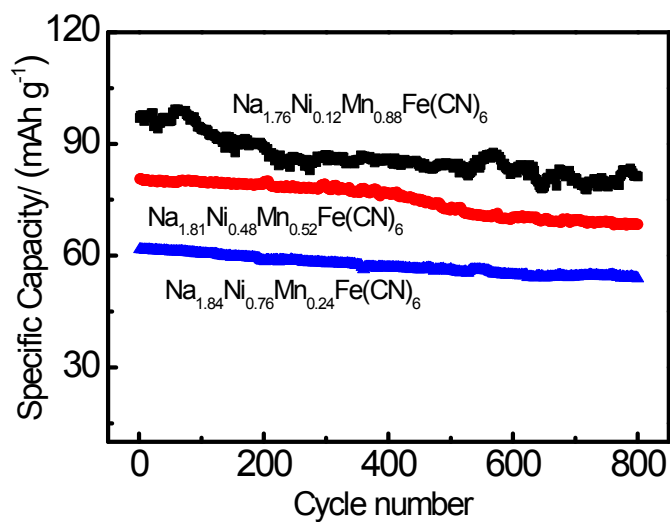


Figure S6. The cycle performances of $\text{Na}_{1.76}\text{Ni}_{0.12}\text{Mn}_{0.88}\text{Fe}(\text{CN})_6$, $\text{Na}_{1.81}\text{Ni}_{0.48}\text{Mn}_{0.52}\text{Fe}(\text{CN})_6$ and $\text{Na}_{1.84}\text{Ni}_{0.76}\text{Mn}_{0.24}\text{Fe}(\text{CN})_6$ between 2.0V-4.0V at 100 mA g^{-1} .

S8. The electrochemical performances of hard carbon electrode

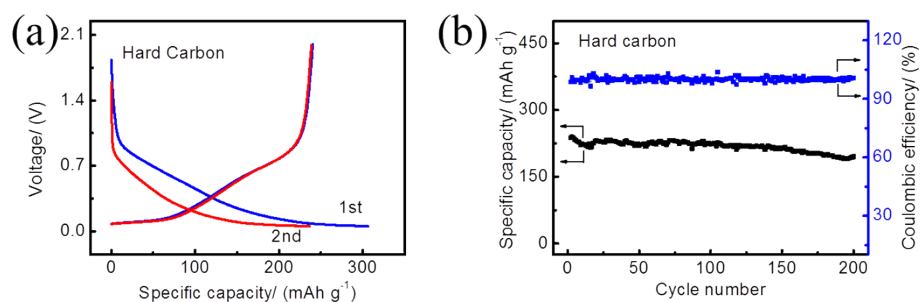


Figure S7. (a): The initial and second charge–discharge profiles, and (b): Cyclic performances of hard carbon between 0.05V-2.0V at 25 mA/g.